Practical Implementation of Lattice QCD Simulation on SIMD Machines with Intel AVX-512[*]

Issaku Kanamori[1] and Hideo Matsufuru[2]

[1] Department of Physical Science, Hiroshima University,
Higashi-hiroshima 739-8526, Japan
`kanamori@hiroshima-u.ac.jp`
[2] High Energy Accelerator Research Organization (KEK),
1-1 Oho, Tsukuba, Ibaraki 305-0801, Japan
`hideo.matsufuru@kek.jp`

Abstract. We investigate implementation of lattice Quantum Chromo-dynamics (QCD) code on the Intel AVX-512 architecture. The most time consuming part of the numerical simulations of lattice QCD is a solver of linear equation for a large sparse matrix that represents the strong interaction among quarks. To establish widely applicable prescriptions, we examine rather general methods for the SIMD architecture of AVX-512, such as using intrinsics and manual prefetching, for the matrix multiplication. Based on experience on the Oakforest-PACS system, a large scale cluster composed of Intel Xeon Phi Knights Landing, we discuss the performance tuning exploiting AVX-512 and code design on the SIMD architecture and massively parallel machines. We observe that the same code runs efficiently on an Intel Xeon Skylake-SP machine.

1 Introduction

Quantum Chromodynamics (QCD) is the fundamental theory to describe the strong interaction among quarks. QCD plays a crucial role not only in understanding the properties of nucleons but also in seeking for new fundamental physics behind the background of QCD through precise theoretical calculation. Because of its nonlinear nature and large coupling at low energy, however, QCD is generally not solved even though the fundamental equation is known. Lattice QCD, which formulates QCD on Euclidean 4-dimensional spacetime lattice, provides a numerical method to tackle this problem [1]. Based on the path integral formulation of quantum field theory, the partition function becomes similar to that of the statistical mechanics so that the Monte Carlo methods are applicable. Typically the most time consuming part of the lattice QCD simulations is solving a linear equation for a large sparse fermion matrix that represents the interaction among quarks. The numerical cost grows rapidly as increasing the

---

lattice size toward precision calculation. Thus the lattice QCD simulations have been a typical problem in high performance computing and progressed keeping step with development of supercomputers.

One of the trends in high performance computer architecture is to possess long SIMD vector registers. The Intel Xeon Phi series is the first product of Intel that has a SIMD vector of 512-bit length. Its second generation, the Knights Landing (KNL) adopts the AVX-512 instruction set. This new instruction set is now available also on the Intel Xeon Skylake-SP series.

In this paper, we port a lattice QCD simulation code to machines composed of KNL and Skylake-SP processors. The aim of this work is to establish techniques to exploit AVX-512, or more generally SIMD architecture, that are applicable to wide range of applications. Since one frequently needs to port a legacy code to a new architecture, it is important to acquire such simple prescriptions to achieve acceptable (not necessarily the best) performance. It is also helpful for designing code structure in future development. For this reason, we restrict ourselves in rather general prescriptions: change of data layout, application of Intel AVX-512 intrinsics, and prefetching. As a testbed of our analysis, we choose two types of fermion matrices together with an iterative linear equation solver. In our previous report [2,3], we developed a code along the above policy and applied it to KNL. In this paper, in addition to improved performance, we rearrange these prescriptions so that each effect is more apparent. As for the fermion matrices, one of those adopted in [2,3] is replaced with other widely used matrix, aiming at extending application of the developed techniques. As a new target machine, we examine a cluster system composed of the Intel Skylake-SP processor.

Here we briefly summarize related works. Since the Skylake-SP is rather new, works related to lattice QCD are so far for KNL. In a KNL textbook [4], Chapter 26 is devoted to performance tuning of the Wilson-Dslash operator (one of matrices examined in this work) using the QPhiX library [5]. Ref. [6] developed a library named 'Grid' for the SIMD architecture, which has largely affected our work. In Ref. [7], through the discussion of memory page granularity, Grid is examined on the Skylake-SP system. A quite large scale test with a preconditioned clover-type fermion matrix is reported in [8]. A pragma-based recipe is examined in [9]. A plenary review at the annual lattice conference [10] summarizes recent activities in lattice QCD community.

This paper is organized as follows. The next section briefly introduces the linear equation system in lattice QCD simulations with fermion matrices employed in this work. Features of the AVX-512 instruction set and our target architectures are summarized in Section 3. Section 4 describes the details of our implementation. We examine the performance of our code on the systems composed of KNL and Skylake in Sections 5 and 6, respectively. We conclude by discussing implication of our results in the last section.

2 Lattice QCD Simulation

For the formulation of lattice QCD and the principle of numerical simulation, there are many textbooks and reviews [1]. Thus we concentrate on the linear equation for the fermion matrix to which high computational costs are required.

The lattice QCD theory consists of fermion (quark) fields and a gauge (gluon) field. The latter mediates interaction among quarks and are represented by 'link variable', $U_\mu(x) \in SU(3)$, where $x = (x_1, x_2, x_3, x_4)$ stands for a lattice site and $\mu = 1, 2, 3, 4$ is the spacetime direction. In numerical simulations the lattice size is finite: $x_\mu = 1, 2, \ldots, L_\mu$. The fermion field is represented as a complex vector on lattice sites, which carries 3 components of 'color' and 4 components of 'spinor', thus in total 12, degrees of freedom on each site. The dynamics of fermion is governed by a functional $S_F = \sum_{x,y} \psi^\dagger(x) D[U]^{-1}(x, y) \psi(y)$, where $D[U]$ is a fermion matrix acting on a fermion vector $\psi(x)$. A Monte Carlo algorithm is applied to generate an ensemble of the gauge field $\{U_\mu(x)\}$, that requires to solve a linear equation $x = D^{-1}\psi$ many times.

There is a variety of the fermion operator $D[U]$, since its requirement is to coincide with that of QCD in the continuum limit, the lattice spacing $a \to 0$. Each formulation has advantages and disadvantages. As a common feature, the matrix is sparse because of the locality of the interaction. In this paper, we examine the following two types of fermion matrix.

Wilson Fermion Matrix The first one called the Wilson fermion matrix has the form

$$D_{\mathrm{W}}(x, y) = \delta_{x,y} - \kappa \sum_{\mu=1}^{4} \left[(1 - \gamma_\mu) U_\mu(x) \delta_{x+\hat{\mu},y} + (1 + \gamma_\mu) U_\mu^\dagger(x - \hat{\mu}) \delta_{x-\hat{\mu},y} \right], \ (1)$$

where x, y are lattice sites, $\hat{\mu}$ the unit vector along μ-th axis, and $\kappa = 1/(8 + 2m_0)$ a parameter related to the quark mass m_0. Fig. 1 indicates how the interaction to the neighboring sites is involved in the matrix. As mentioned above, the link variable $U_\mu(x)$ is a 3×3 complex matrix acting on the color and γ_μ is a 4×4 matrix acting on the spinor degrees of freedom. Thus D_{W} is a complex matrix of the rank $4N_c L_x L_y L_z L_t$. It is standard to impose the periodic or anti-periodic boundary conditions.

Clover Fermion Matrix The second fermion matrix called 'clover' fermion is an improved version of the Wilson fermion so as to reduce the discretization error. It is widely used in practical simulation due to its moderate numerical cost. The clover fermion matrix is defined as

$$D_{\mathrm{clov}}(x, y) = D_{\mathrm{W}}(x, y) + F(x) \delta_{x,y}, \tag{2}$$

where $F(x)$ in the additional term is a 12×12 Hermitian matrix made of link variables. By choosing a proper basis, $F(x)$ is represented as a block diagonal
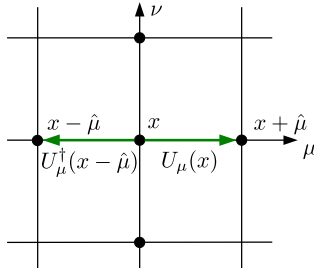
Fig. 1. The schematic feature of the Wilson fermion matrix

Table 1. Features of the fermion matrices: The number of floating point operations and the data transfer between memory and processor per site. The so-called roofline estimates for the Oakforest-PACS (roofline 1) and ITO (roofline 2) are obtained from the values of Byte/Flop. The ideal cases assume that the data are loaded from the memory only once.

Fermion type	N_{flop}/site	data/site float [B]	Byte/Flop	roofline 1 (ideal) [GFlops]	roofline 2 (ideal) [GFlops]
Wilson	1368	1536	1.12	424 (1350)	228 (729)
Clover	1944	1824	0.94	506 (1200)	273 (648)

form with two 6×6 Hermitian matrices. Note that $F(x)$ is determined before the solver algorithm is applied and stored as an array data similarly to the link variable $U_\mu(x)$ so that its building cost is ignored in this paper.

The above two fermion matrices have differences in data size transferred between the memory and the processor cores, and number of arithmetic operations. Table 1 summarizes these values per site for single precision data. As quoted in Table 1, the clover matrix tends to have smaller byte-per-flop value, due to the multiplication of $F(x)$. With caches one can expect reuse of data. Every link variable $U_\mu(x)$ and vector on each site can be reused maximally two and nine times, respectively. In the ideal case, byte-per-flop ratio becomes 0.351 and 0.395 for the Wilson and clover matrices, respectively. The ratio becomes larger for the clover matrix since $F(x)$ is used only once. The last two columns in Table 1 are so-called roofline estimates, the performance limit determined by the memory bandwidth, for our target machines, Oakforest-PACS and ITO. For the former, the bandwidth of the MCDRAM is used. The ideal roofline is estimated by assuming that the data are loaded from the memory only once and successive access is to the cache.

As mentioned above, we need to solve a linear equation system with the fermion matrix. Since the fermion matrices are large and sparse, iterative solvers based on the Krylov subspace method are widely used. We employ the BiCGStab algorithm for a non-Hermitian matrix. We focus on the performance with single precision, since it is practically used as an inner solver of a mixed precision solver and governs the performance of the whole solver. While there are variety

of improved solver algorithms for a large-scale linear systems, such as a multi-grid or domain-decomposition methods, they are beyond the scope of this paper.

3   Target Architectures

Our target architectures adopt the Intel AVX-512 instruction set. Each thread can use 32 vector registers of 512-bit length which can process 16 single or 8 double precision floating point numbers simultaneously. A fused multiplication and add (FMA) operation on SIMD registers can perform 32 FLOPs (single precision) and 16 FLOPs (double). The full instruction set consists of several sub-categories among which all the processor launched so far can exploit AVX-512F (Foundation) and AVX-512CD (Conflict Detection).

Knights Landing The first example with AVX-512 is the Intel Xeon Phi Knights Landing (KNL). It is the second generation of Intel Xeon Phi architecture, whose details are found in [4]. It is composed of maximally 72 cores, in units of a tile that is composed of two cores sharing distributed L2 cache. Each core supports 4-way hyper-threading. In addition to DDR4 memory with about 90 GB/s, MCDRAM of maximally 16 GB accessible with 475–490 GB/s [11] is available with one of three modes: cache, flat, and hybrid. Our target machine with KNL is the Oakforest-PACS system hosted by Joint Center for Advances High Performance Computing (JCAHPC, University of Tokyo and University of Tsukuba). The system is composed of 8208 nodes of Intel Xeon Phi 7250 (68 cores, 1.4 GHz) connected by full-bisection fat tree network of the Intel Omni-Path interconnect. It has 25 PFlops of peak performance in total, and started public service in April 2017.

Skylake-SP The AVX-512 instruction set has become available on the new generation of Intel Xeon processor, Skylake-SP. We use a system named ITO at the Research Institute for Information Technology, Kyushu University. It started full operation in January 2018. Each node of ITO has two Intel Xeon Gold 6154 (Skylake-SP, 18 cores, 3.0 GHz) processors which amounts to 6.9 TFlops/node of peak performance in single precision (slightly larger than single KNL node). The main difference from KNL is the memory structure: instead of MCDRAM, Skylake-SP has a L3 cache. It is shared by all cores in CPU and its size is 24.75MB. The bandwidth of the main memory (DDR4, 192 GB/node) is 255.9 GB/s/node.

4   Implementation

Our base code is the Bridge++ code set [12,13] which is described in C++ based on an object oriented design and allows us to replace fermion matrices and solver algorithms independently. In the original Bridge++, hereafter called the Bridge++ core library, the data are in double precision and in a fixed data

layout with array of structure (AoS). Following the strategy employed in [14], we extend Bridge++ to enable a flexible data layout and an arbitrary precision type. The key ingredients of our implementation are as follows: changing data layout, use of intrinsics, manual prefetching, assignment of the thread tasks. In the following, these issues are described in order in some detail.

Data Layout It is important to choose a proper data layout to attain high affinity to the SIMD vector registers. As a 512-bit register corresponds to 8 or 16 floating point numbers in double and single precision, respectively, we rearrange the date in these units. We implement the code in C++ template classes and instantiate them for the double and float data types individually. There are several ways in ordering the real and imaginary parts of complex variables. Considering the number of SIMD registers and the number of the degree of freedom on each site, we decide to place the real and imaginary parts as consecutive data on the memory. The color and spinor components are distributed to separate registers. Instead several sites are packed into a SIMD vector; complex variables of float (double) type on eight (four) sites are processed simultaneously. To allocate the data on the memory, we use `std::vector` in the standard C++ template library with providing an aligned allocator.

There is still flexibility in folding the lattice sites into a data array. We compare two different data layouts displayed in Fig. 2. To avoid lengthy description, we assume the single precision case in the following. In the first case (layout 1), several sites in x-coordinate composes a SIMD vector. This requires the local lattice size in x-direction to be a multiple of eight. Since the x-coordinate is the most inner coordinate of our index, it is a simplest extension of a non-vectorized layout. To minimize performance penalty of boundary copy, the MPI parallelization is not applied in x-direction.

The second layout (layout 2) was introduced in Ref. [6]. As the right panel of Fig. 2 explains, the local lattice is divided into several subdomains each provides one complex number to one SIMD vector. With our implementation this restricts the local lattice sizes in y-, z-, and t-directions to be even. While there is no restriction in x-direction for layout 2, throughout this paper we do not MPI parallelize in x-direction similarly to the layout 1.

Using Intrinsics The arithmetic operations on the SIMD variables are explicitly managed using the intrinsics. We wrap them in inline functions, which cover common basic operations such as complex four arithmetic operations and BLAS-like functions (axpy, etc.). By replacing the wrapper function, our code can be easily adapted to other architectures such as AVX2. We partially make use of the `simd` directory in the Grid library [6] that provides similar wrappers. Defining types that wrap the 512-bit SIMD vectors (`__m512` or `__m512d`) and using arrays of them, the compiler generates a load/store instruction for a vector register. We therefore do not explicitly use load or store intrinsics, except for streaming stores.
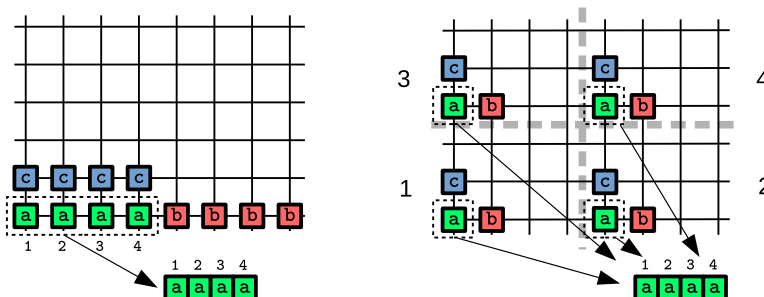
Fig. 2. The site index ordering for the layout 1 (left) and 2 (right) in the double precision case. We use a three-dimensional analogues of the right panel for the layout 2 in single precision.

Prefetching We compare the manual prefetch and the automated prefetch by compiler. The most outer loop of the matrix is for the site index (modulo SIMD vector). At each site, one accumulates nine stencil contributions, from $+x$, $-x$,...,$-t$ directions in order, and of that site. It turned out that in most cases only the prefetch to L2 cache is relevant. Manual prefetch to L1 cache sometimes causes slowing down[3]. The prefetch to L2 cache is inserted at three steps before the computation except for the contributions from the $-x$ direction and that site. Since x is the innermost site index, the neighboring data in $-x$ direction most likely remain in the cache. For the clover fermion matrix, additionally two 6×6 block matrices in the clover term $F(x)$ are multiplied. The prefetch is applied only to the first block matrix. To trigger the hardware prefetch, a few more prefetches to L1 cache are inserted: (i) at the beginning of the site loop in order to load the data in $+x$ direction, and (ii) at the almost end of multiplication of the first block matrix of the clover term to load the second block matrix. We also insert several L2 and L1 prefetches during the packing of data for communication and index calculation so as to load the local lattice sizes.

We use **_mm_prefetch** with **_MM_HINT_T0** and **_MM_HINT_T1** to generate the prefetch order. The following pseudo-code is an example of prefetch insertions.

```
for(s=0; s<num_of_sites; s++){
#pragma noprefetch
  // +x
  prefetch_to_L1(+x);
  prefetch_to_L2(-y);
  accumulate_from(+x);
  // -x
  prefetch_to_L2(+z);
  accumulate_from(-x);
  // +y
  prefetch_to_L2(-z);
```

---

[3] Removal of such prefetch is one of the reasons of improved performance from our previous report [3].

```
  accumulate_from(+y);

  ...
}
```

It is not straightforward to insert prefetch commands appropriately. One needs to tune the variables and the place to insert referring to a profiler, *e.g.* Intel Vtune amplifier. The performance may be sensitive to the problem size, choice of parameters such as the number of threads, and so on.

Thread Task Assignment Since the lattice usually extends over at least several nodes, a multiplication of matrix requires communication among nodes. The matrix multiplication has the following steps in order: (1) Packing of the boundary data for communication, (2-a) Doing communication, (2-b) Operations of the bulk part, and (3) Unpacking the boundary data and operations on the boundary part. (2-a) and (2-b) can be overlapped, and its efficiency is the key for the total performance. We restrict ourselves in the case that only the master thread performs the communication, *i.e.* corresponding to `MPI_THREAD_FUNNELED`. For the implementation of the steps (2-a) and (2-b) above, there are two possibilities: (i) arithmetic operational tasks are equally assigned to all the available threads, and (ii) the master thread concentrates the communication and other threads bear the arithmetic tasks. We adopt the case (ii) in this work, since it tends to be faster.

In order to make the extrapolation of the scaling easier, we always enforce the above communication procedure in all the y-, z- and t-directions even if no MPI parallelization is imposed, so that the "communication" may just result in a copy of packed data.

5   Performance on KNL Machine: Oakforest-PACS

5.1   Machine Environment

We start with tuning on Oakforest-PACS. We use the Intel compiler of version 18.0.1 with options `-O3 -ipo -no-prec-div -xMIC-AVX512`. On execution, job classes with the cache mode of MCDRAM are used. According to the tuning-guide provided by JCAHPC, we adopt the following setup. To avoid OS jitters, the 0th and 1st cores on each KNL card are not assigned for execution. `KMP_AFFINITY=compact` is set if multiple threads are assigned to a core (unset for 1 thread/core).

5.2   Matrix Multiplication

Vector Variables We first compare our new implementation with the core library of Bridge++, which does not explicitly use the vector variables. Fig. 3 shows the performance of the Wilson matrix multiplication in double precision on a single node. We use the layout 1 for the new code as it has similar site
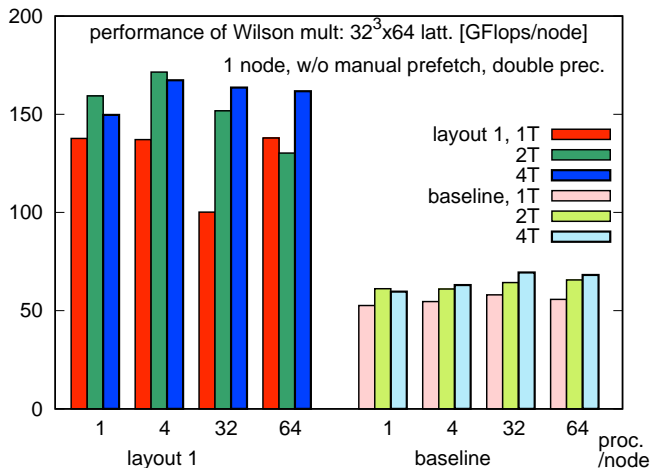
Fig. 3. Effect of using the SIMD vector variables: the performance of the Wilson matrix multiplication on a single KNL node.

layout on the memory. The new code (layout 1) exhibits 2–3 times better performance than the core library (baseline). We also observe that the new code has a strong dependence on the number of hyper-threading (denoted by 1T–4T). As shown later, the best performance is achieved with 2T in most cases for the new implementation.

Data Layout Fig. 4 compares the layout 1 and 2 for the Wilson matrix multiplication. In this result the layout 1 is always faster. A presumable reason is an extra shuffle inside the SIMD vector for the layout 2 at the boundary of the local lattice in y-, z- and t-directions. In the current implementation of layout 2, the data are always once shuffled even in the bulk and then a mask operation chooses shuffled or unshuffled data. Such a conditional shuffling does not exist in the layout 1. Another possible reason is that, in packing the data for communication, the layout 2 uses only the half of data in a SIMD vector. Converting two SIMD vectors into one causes additional instructions and additional load from the memory.

As apparent in Fig. 4 and successive two figures, the performance depends on the number of hyper-threads/core while no general tendency is observed. Since it can be easily changed at run time, hereafter we focus on the best performance case without indicating the number of hyper-threads.

Prefetching Effect of the manual prefetch against the automated prefetch by compiler is displayed in Fig. 5. On a single node, where no inter-node communication is needed, the manual prefetch achieves substantial improvement. In the maximum performance case (4 MPI process) its effect is more than 10%,
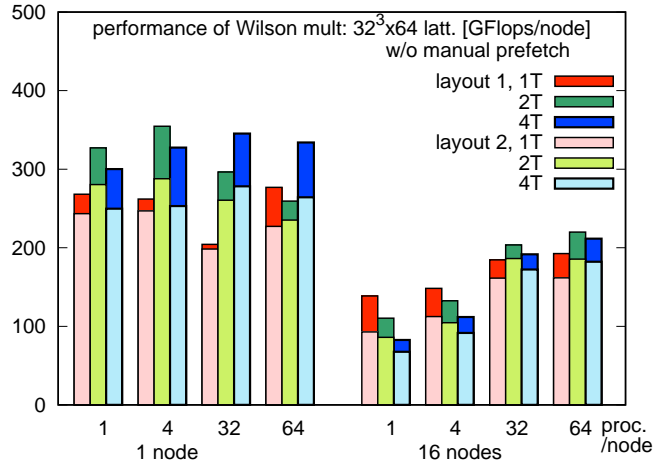
Fig. 4. Data layout dependence: performance of the Wilson matrix multiplication without prefetch on a single KNL node.

from 355 to 404 GFlops. In some cases more gains are obtained. Increasing the number of nodes, however, the effect is gradually washed out and becomes only a few percent at 16 nodes in the cases of 32 and 64 processes/node. Sometimes the manual prefetch even slightly reduces the performance, for which the colors are flipped in Fig. 5. We observe a similar improvement for the clover matrix multiplication: from 413 to 475 GFlops on single node (4 MPI proc./node) and from 277 to 287 GFlops/node on 16 nodes (64 proc./node).

Since our target lattice sizes assume more than $O(10)$ KNL nodes, the advantage of manual prefetch is not manifest compared to involved tuning effort. In the following, we nonetheless use the code with manual prefetches. The performance without manual prefetch may be estimated based on the result in Fig. 5.

For reference, here we quote the effect of communication overhead for a single MPI process case on a single node. As noted above, even in such a case the copy of packed boundary data is performed. By removing the redundant boundary data packing and copy, the performance changes as follows: $378 \rightarrow 453$ GFlops (layout 1) and $345 \rightarrow 361$ GFlops (layout 2) for the Wilson matrix, and $430 \rightarrow 497$ GFlops (layout 1) and $388 \rightarrow 440$ GFlops (layout 2) for the clover matrix multiplication.

Comparison to Other Codes Now we compare our performance of the Wilson and clover matrix multiplication to other codes under the condition of a single process on a single KNL node. The QPhiX library achieves 587 GFlops for single precision [4] on a $32^3 \times 96$ lattice. The Grid library [6] provides a benchmark of the Wilson matrix that we can run on the same environment as this work. On a $32^3 \times 64$ lattice, based on v0.7.0, it gives the best performance with one thread/core and amounts to 340 GFlops that is comparable to our result.
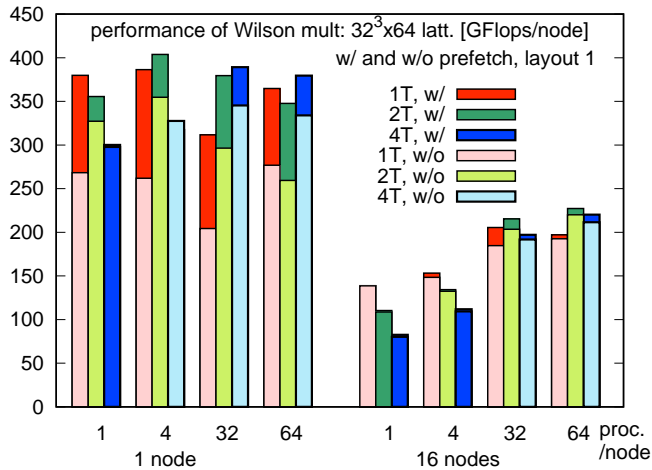
Fig. 5. Effect of prefetch: performance of the Wilson matrix multiplication with the layout 1 on a single KNL node.

According to Ref. [10], the Grid achieves 960 GFlops with multiple right hand sides, that has an advantage in reuse of data. While our result is not as fast as QPhiX, it shows that large fraction of performance can be achieved with rather simple prescriptions. An approach keeping the array of structure data layout and inserting pragmas [9] gives 225 GFlops (245 GFlops after correcting the difference in clock cycle). In our previous report [3], which corresponds to the layout 2 without redundant boundary data packing/copy, the best performance on single node was 340 GFlops (4 MPI proc./node). With the same condition, it becomes 369 GFlops whose improvement is mainly due to the refinement of the prefetch. Boku *et al.* [8] reported that on the same machine an even-odd preconditioned clover matrix multiplication, which adopts different implementation from ours with the smaller byte-per-flop value of 0.645, runs with about 560 GFlops/node up to 8,000 KNL nodes. The multi-node result with Grid reported in [7] is 277 GFlops with a local lattice volume 24^4.

Scaling Property of Matrix Multiplication Fig. 6 shows the weak scaling property up to 32 nodes for the Wilson (left) and the clover (right) matrix multiplication with a local lattice volume 32×16^3. The values are measured by averaging over successive 1,000 multiplications. As expected from the byte-per-flop values, the clover matrix is more efficient than the Wilson matrix. For both the matrices, better performance is observed for 32 or 64 MPI processes per node (1 process per tile or core) than the other two cases. A similar tendency is observed in Fig. 5, which corresponds to a strong scaling from 1 node to 16 nodes with a lattice volume $32^3 \times 64$.
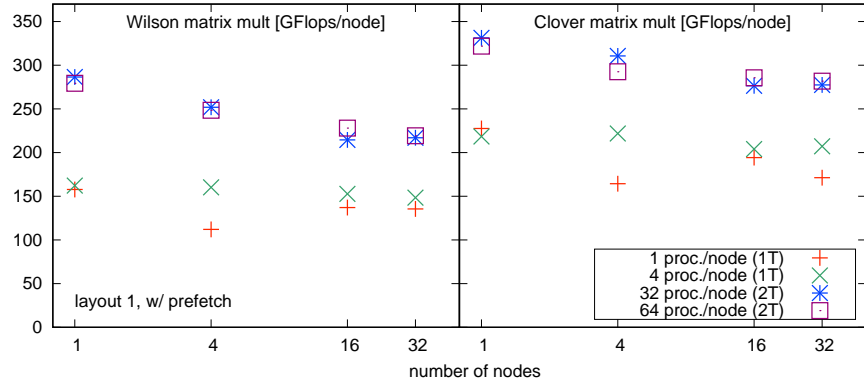
Fig. 6. Weak scaling plots for the matrix multiplication with a 32×16^3 local lattice in each node measured on Oakforest-PACS.

5.3 Performance of BiCGStab Solver

For both the Wilson and clover matrices, the BiCGStab solver works efficiently. We compose the solver algorithm with BLAS-like functions to which neither manual prefetch nor additional compiler option for prefetch is applied. In Fig. 7, we show the weak scaling plot of performance for the BiCGStab solver with the Wilson and clover matrices. The performance is an average over 12 times of solver call for different source vectors. Because of larger byte-per-flop values of the linear algebraic functions, the performance reduces to about half the matrix multiplication at 32 nodes[4]. Currently, each BLAS-like routine independently executes a load and store of data. Fusing several functions may improve the performance.

6 Performance on Skylake-SP: ITO

Machine Environment Another machine we examine is ITO at Kyushu University. The Intel compiler of version 18.0.0 is used with the options `-ipo -O3 -no-prec-div -fp-mpdel fast=2 -xHost`. At run time an environment variable `KMP_AFFINITY=compact` is set.

Tuning We do not apply additional code tuning. Actually, as shown below, the code tuned for KNL works reasonably well on the Skylake-SP machines. The effect of the manual prefetch, however, is quite limited or even negative. While refining prefetch tuning properly to the Skylake-SP processor might improve the performance, we abandon to apply it. We also observe that using hyper-threading

---

[4] The BiCGStab performance in the previous report [3] was about the half of the actual one, due to a bug in counting the matrix multiplications.
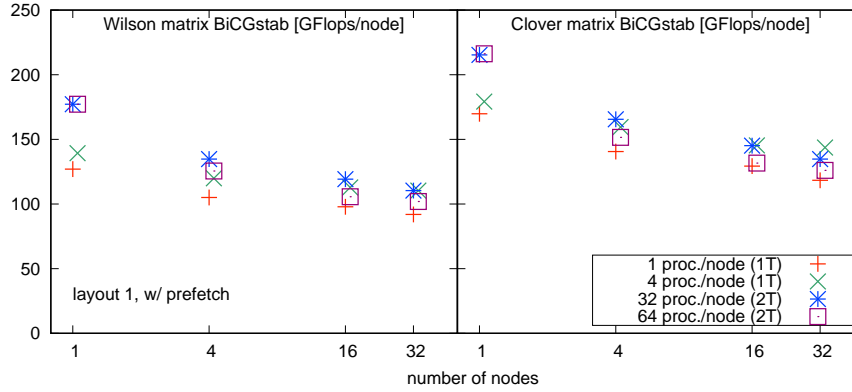
Fig. 7. Weak scaling plots for the BiCGStab solver with the Wilson and clover matrices with a $16^3 \times 32$ lattice in each node measured on Oakforest-PACS. Some symbols are slightly shifted horizontally to improve the visibility.

— up to 2 hyper-threads are possible — spoils the performance significantly, and thus do not use it.

Matrix Multiplication Fig. 8 shows the weak scaling property of the matrix multiplication up to 16 nodes. In the top panel the lattice volume per node is $32 \times 16 \times 12 \times 12$, which is chosen to allow 36 MPI processes per node. We observe the performance with 36 MPI proc./node is much higher than the other two cases. The single node performance is 669 GFlops for the Wilson and 625 GFlops for the clover matrices, which is 91.8% and 96.5% of the roofline limit of the ideal data reusing, respectively. This implies that because of the small local lattice volume reuse of data on cache is almost perfect. As expected from the roofline estimate, the Wilson matrix exhibits better performance than the clover matrix. Increasing the lattice volume per node to 64×32^3, such high performance is lost as shown in the bottom panel of Fig. 8. The performance of the Wilson matrix multiplication is 230 GFlops, which is slightly above the roof line estimation without any data reuse. Note that the 2 proc./node result in the top panel of Fig. 8 is 243 GFlops.

Another observation is that the case with single MPI process per node is the slowest. Since in our implementation the communication is performed by the master thread and other threads take charge of arithmetic operations, the communication load becomes more significant as the total number of threads per process increases. In fact, for a single MPI process on single node, removing redundant boundary data copy results in significant increase of performance: 249 $\rightarrow$ 767 GFlops for the Wilson and 306 $\rightarrow$ 624 GFlops for the clover matrices on the $32 \times 16 \times 12 \times 12$ lattice. By replacing the MPI function with a substitution parallelized with threads, the performance becomes about 80% of that without copy of packed data. This implies that one or a few process(es) per node is less
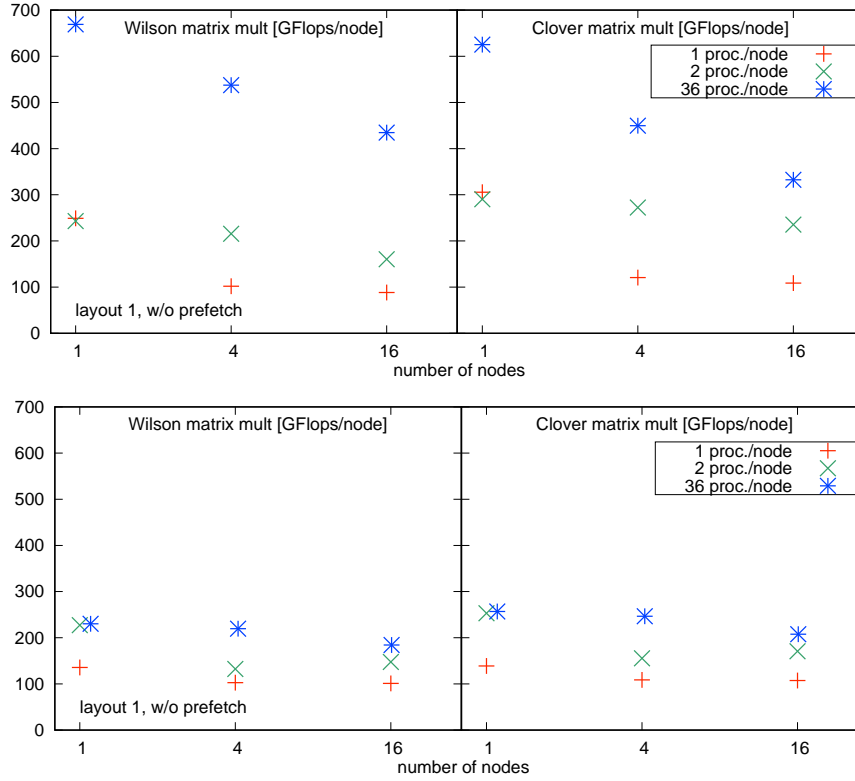
Fig. 8. Weak scaling plots for the Wilson and clover matrix multiplication on ITO. The local lattice sizes on each node are $32 \times 16 \times 12 \times 12$ (top panel) and $64 \times 32 \times 24 \times 24$ (bottom).

efficient as the local lattice size increases. The performance of the Wilson matrix without boundary copy exceeds the roofline estimate with ideal reuse of cached data. This may indicate that the data on the cache partially remain until the next multiplication of the matrix.

BiCGStab Solver Fig. 9 shows the weak scaling of the BiCGStab solver with a $32 \times 16 \times 12 \times 12$ local lattice per node. Again we observe high performance in the 36 proc./node case, which is better than the result on single KNL node. Because of higher requirement for the bandwidth in the linear algebra, however, the performance is less than the matrix multiplication. As observed in the matrix multiplication, launching one MPI process per core achieves the best performance.
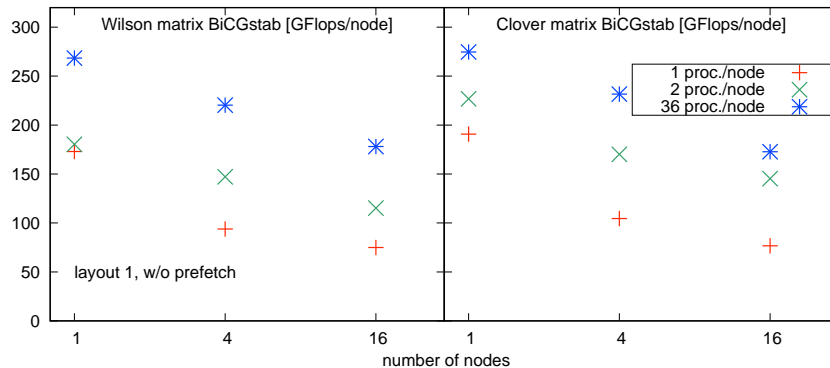
Fig. 9. Weak scaling plots for the BiCGStab solver with the Wilson and clover matrices with a $32 \times 16 \times 12 \times 12$ local lattice in each node measured on ITO.

7 Conclusion

In this paper, we applied rather simple prescriptions to make use of the SIMD architectures with the Intel AVX-512 instruction set to a typical problem in lattice QCD simulation. Two different types of cluster systems were examined, one composed of Intel Xeon Phi Knights Landing and the other of Intel Xeon Skylake-SP. We examine mainly the following prescriptions: rearrangement of data layout, use of the AVX-512 intrinsics, and manual prefetching. The former two are crucial to achieve acceptable performance. Not only to employ vector type variables, we compare two data layouts and found the layout 1 achieves better performance by about 10–20%, while constraint on the MPI parallelization is slightly stronger than the layout 2. The effect of manual prefetching is more restrictive. It is worth paying dedicated effort only on single or small number of KNL nodes.

The same code is examined on a cluster system composed of Skylake-SP. We observed that the code tuned for KNL exhibits a reasonable performance, while the prefetch provides almost no effect. If one chooses the lattice size and number of nodes appropriately so that the problem size in each node is small enough, high performance is expected by efficient reuse of cached data. Since the L3 cache of Skylake-SP is faster than the MCDRAM of KNL, it would be more effective to apply cache tuning, such as loop tiling. For both the systems of KNL and Skylake-SP, we conclude that running as a massive parallel machine is the efficient way.

Acknowledgment

References

1. For modern textbooks, *e.g.*, DeGrand, T., C. DeTar, C.: Lattice Methods for Quantum Chromodynamics. World Scientific Pub., (2006); Gattringer C., Lang C. B.: Quantum Chromodynamics on the Lattice. LNP, vol 788. Springer, Berlin Heidelberg (2010). doi:10.1007/978-3-642-01850-3
2. Kanamori, I., Matsufuru, H.: Wilson and Domainwall Kernels on Oakforest-PACS. EPJ Web Conf. **175**, 09002 (2018). doi:10.1051/epjconf/201817509002 [arXiv:1710.07226 [hep-lat]].
3. Kanamori, I., Matsufuru, H.: Practical Implementation of Lattice QCD Simulation on Intel Xeon Phi Knights Landing. In: 2017 Fifth International Symposium on Computing and Networking (CANDAR), pp. 375–381, IEEE Explore (2018). doi:10.1109/CANDAR.2017.66 [arXiv:1712.01505 [hep-lat]].
4. Jeffers J., Reinders, J., Sodani A.: Intel Xeon Phi Processor High Performance Programming Knights Landing Edition. Morgan Kaufmann, Cambridge (2016)
5. QPhiX library, `https://github.com/JeffersonLab/qphix`
6. Boyle, P. A., Cossu, G., Yamaguchi, A., Portelli, A.: Grid: A next generation data parallel C++ QCD library. PoS LATTICE **2015**, 023 (2016). doi: 10.22323/1.251.0023 [arXiv:1512.03487 [hep-lat]].
7. Boyle, P., Chuvelev,M., Cossu, G., Kelly, C., Lehner ,C. and Meadows, L.: Accelerating HPC codes on Intel(R) Omni-Path Architecture networks: From particle physics to Machine Learning, arXiv:1711.04883 [cs.DC]
8. Boku, T., Ishikawa, K.-I., Kuramashi, Y., and Meadows, L.: Mixed Precision Solver Scalable to 16000 MPI Processes for Lattice Quantum Chromodynamics Simulation on the Oakforest-PACS System. In: 2017 Fifth International Symposium on Computing and Networking (CANDAR), pp. 362–368 (2018), IEEE Explore (2018). doi:10.1109/CANDAR.2017.69 [arXiv:1709.08785 [physics.comp-ph]].
9. Durr, S.: Optimization of the Brillouin operator on the KNL architecture. EPJ Web Conf. **175**, 02001 (2018). doi:10.1051/epjconf/201817502001 [arXiv:1709.01828 [hep-lat]].
10. Rago, A.: Lattice QCD on new chips: a community summary EPJ Web Conf. **175**, 01021 (2018). doi:10.1051/epjconf/201817501021 [arXiv:1711.01182 [hep-lat]].
11. Raman, K. (Intel), Optimizing Memory Bandwidth in Knights Landing on Stream Triad. `https://software.intel.com/en-us/articles/optimizing-memory-bandwidth-in-knights-landing-on-stream`
12. Bridge++ project. `http://bridge.kek.jp/Lattice-code/`
13. Ueda, S. *et al.*: Bridge++: an object-oriented C++ code for lattice simulations. PoS LATTICE2013, 412 (2014). 10.22323/1.187.0412.
14. Motoki, S. *et al.*: Development of Lattice QCD Simulation Code Set on Accelerators. Procedia Computer Science **29**, pp. 1701–1710 (2014).

doi:10.1016/j.procs.2014.05.155; Matsufuru, H. *et al.*: OpenCL vs OpenACC: Lessons from Development of Lattice QCD Simulation Code. Procedia Computer Science **51**, pp. 1313-1322 (2015). doi:10.1016/j.procs.2015.05.316